193. Quantitative Line-Shape Analysis of Temperature- and Concentration-Dependent ^{13}C-NMR Spectra of ^{6}Li- and ^{13}C-Labelled Organolithium Compounds

Kinetic and Thermodynamic Data for Exchange Processes in Dibromomethyllithium, (Phenylthio)methyllithium, and Butyllithium

by **Josef Heinzer, Jean F. M. Oth,** and **Dieter Seebach***

Laboratorium für Organische Chemie der Eidgenössischen Technischen Hochschule, ETH-Zentrum, Universitätstrasse 16, CH-8092 Zürich

(19.VII.85)

Using the 'permutation of indices' method proposed by *Kaplan* and *Fraenkel*, we could formulate the density-matrix equations required to fit the temperature-dependent ^{13}C-NMR spectra observed with the title compounds. For $^{6}Li^{13}CHBr_2$ (**1**) and $^{6}Li^{13}CH_2SC_6H_5$ (**2**) an exchange mechanism is proposed by which monomers interchange C- and Li-atoms *via* a non-observed dimeric intermediate; the activation parameters of these intermolecular dynamic processes have been found to be $\Delta H^{\neq} = 10.2$ kcal/mol, $\Delta S^{\neq} = 13.7$ cal/mol·K for **1** and $\Delta H^{\neq} = 11.1$ kcal/mol, $\Delta S^{\neq} = 20.6$ cal/mol·K for **2** ((D_8)THF as solvent). In the case of (^{6}Li)butyllithium (**3**), the observed low-temperature spectra indicate that dimeric (**3b**) and tetrameric (**3a**) species are in dynamic equilibrium interchanging the $C_3H_7{}^{13}CH_2$ groups (and THF molecules) bonded to the ^{6}Li-atoms. The relative concentrations of the dimer and of the tetramer have been determined by peak integration or by line-shape fitting; the 'pseudo'-equilibrium constant, defined by $K'_{eq} = [\mathbf{3b}]^2/[\mathbf{3a}]$, was found to be $2.6 \cdot 10^{-2}$ mol/l (at $-88°$) and corresponds to $\Delta G_R(-88°) = 2\,\Delta G_f^{\circ}(\mathbf{3b}) - \Delta G_f^{\circ}(\mathbf{3a}) = 1.34$ kcal/mol. The activation parameters of the dynamic process responsible for the exchange were estimated as $\Delta H^{\neq} = 3.78$ kcal/mol and $\Delta S^{\neq} = -31.3$ cal/mol·K. Tentative interpretation of the thermodynamic and kinetic parameters is given.

1. Introduction. – The interaction of *Lewis* bases with organolithium compounds has been extensively studied by many authors [1]. These investigations have shown that alkyllithiums exist predominantly as hexamers in hydrocarbon solvents and as tetramers and/or dimers in basic solvents. Equilibria between different aggregates have been investigated; even 'calorimetric titration' of organolithium compounds such as BuLi with different bases (including THF) have been carried out [2]. Close inspection of the thermochemical data published in [2] allowed us to conclude that the following reversible reactions occur when pure BuLi dissolved in an apolar solvent is titrated with THF:

$$(RLi)_6 + 2\,THF \rightarrow (RLi)_6 \cdot 2\,THF \qquad \Delta H_R = -14.7\ kcal/mol$$

$$(RLi)_6 \cdot 2\,THF + 4\,THF \rightleftarrows 3/2\,(RLi)_4 \cdot 4\,THF \qquad \Delta H_R = -18.0\ kcal/mol$$

$$(RLi)_4 \cdot 4\,THF + 4\,THF \rightleftarrows 2\,(RLi)_2 \cdot 4\,THF \qquad \Delta H_R = -3.6\ kcal/mol$$

$$(RLi)_2 \cdot 4\,THF + 2\,THF \rightleftarrows 2\,RLi \cdot 3\,THF \qquad \Delta H_R = small$$

From the last two equations and from their corresponding ΔH_R values, one might expect that in pure THF the tetrameric, dimeric, and monomeric forms of BuLi are in dynamic equilibrium.

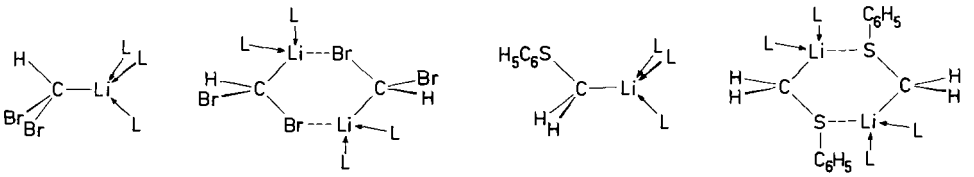

1a **1b** **2a** **2b**

L = oxygen ligand of solvent molecules

One method to investigate the degree of aggregation of alkyllithium derivatives in different types of solvents is to measure the ^{13}C-NMR spectra of ^{6}Li,^{13}C-labelled organolithium compounds. In the course of such measurements, one often observes that singlet signals assigned to the lithiated C-atoms broaden and split up into multiplets upon cooling (below −70°) or upon diluting the solutions at a given low temperature [3] [4]. This implies that intermolecular exchange processes by which a given Li-atom is not permanently bonded to the same C-atom are fast on the NMR time scale and are responsible for the observed line shape. The purpose of this work is to investigate quantitatively these dynamic processes that one observes when the temperature or the concentration of the Li-alkyl derivatives is changed. Assuming an appropriate chemical-exchange model and applying the 'permutation of indices' method of *Kaplan* and *Fraenkel* [5], we were able to derive the density-matrix equations required to simulate the ^{13}C-NMR spectra of (^{6}Li)dibromomethyllithium (**1**; temperature range: −96 to −117°) [3a], of (^{6}Li)(phenylthio)methyllithium (**2**; −100 to −133°) [3c] [3d], and of (^{6}Li)butyllithium (**3**; −30 to −110°, at concentrations 0.1 to 0.5M) [3a] [3e], all these compounds being ^{13}C-labelled (90% ^{13}C) at the lithiated (99.5% ^{6}Li) C-atom. The spectra, previously published, have then been fitted by an appropriate iterative least-squares procedure (program NMREX2).

2. Line-Shape Analysis of the ^{13}C-NMR Signals of ^{6}Li^{13}CHBr$_2$ (1) and ^{6}Li^{13}CH$_2$SC$_6$H$_5$ (2). – At temperatures below −100°, the signals of the lithiated ^{13}C-atoms of compounds **1** and **2** dissolved in (D_8)THF are 1:1:1 triplets with coupling constants $^{1}J(^{13}C,^{6}Li)$ (spin of ^{6}Li = 1) of 16.3 and 10.8 Hz, respectively. This indicates that **1** and **2** are present either as monomeric species (**1a**, **2a**) or as heteroatom-bridged aggregates (**1b**, **2b**). It should be noted here that in the crystalline state, a *N,N,N',N'*-tetramethylethylenediamine (TMEDA) complex of **2** has been shown to be dimeric [6]. So far, the degree of aggregation of **1** in THF solution has not been determined, but **2** was shown by cryoscopy [7] to be mainly monomeric. The triplet ^{13}C-signal observed for each compound coalesces into a singlet without change of chemical shift (**1**: 101.3 ppm; **2**: 3.0 ppm) upon warming the solution. Concentration effects studied on **2** indicate that the coalescence temperature of the triplet ^{13}C-signal increases when the solution is diluted; here again, this change in line-shape occurs without appreciable variation of the resonance position [3c]. These

Scheme 1

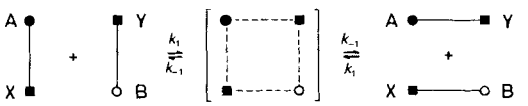

$$AX + BY \overset{k}{\rightleftharpoons} AY + BX \qquad (1)$$

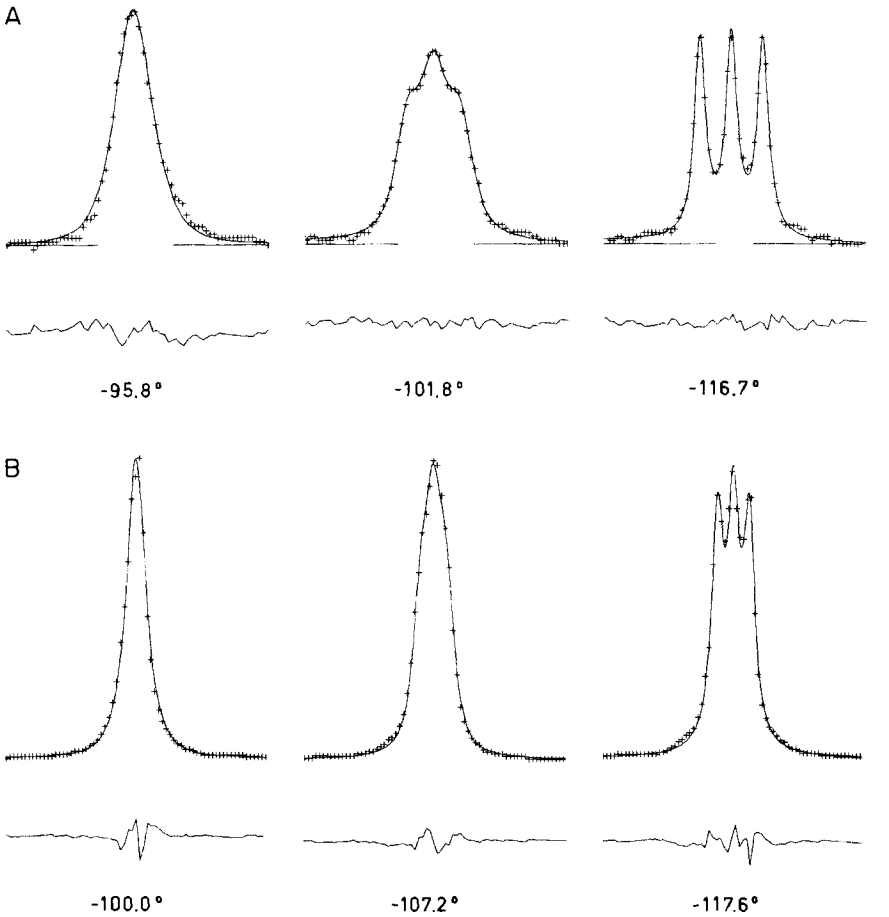

Fig. 1. *Experimental (+) and calculated spectra of* $^{6}Li^{13}CHBr_2$ (**1**; A) *and* $^{6}Li^{13}CH_2SC_6H_5$ (**2**; B). The errors y_i(calc.) − y_i(exp.) are visualized (in the same intensity scale as the spectra) by the noisy lines.

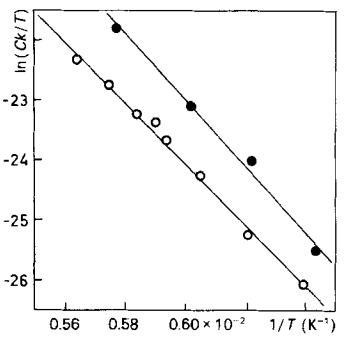

Fig. 2. Eyring *plot of the spin-exchange rates* k *of* $^{6}Li^{13}CHBr_2$ (**1**; ○) *and* $^{6}Li^{13}CH_2SC_6H_5$ (**2**; ●), *respectively.* $C = h/k_b$ with h = *Planck*'s constant and k_b = *Boltzmann*'s constant.

observations are compatible with the mechanism shown in *Scheme 1* where X and Y are individualized Li-atoms and A and B individualized ^{13}C-atoms.

The density-matrix equations can be derived (see *Appendix A*) by considering the spin exchange associated with the overall reaction formulated by *Eqn. 1*; the exchange parameters are then obtained by an iterative line-shape-fitting procedure using the program NMREX2 (briefly described in the *Appendix B*). In *Fig. 1A* and *1B*, the signals from the lithiated ^{13}C-atoms of **1** and **2** observed at three different temperatures are compared with the calculated line-shapes. It is to be noted that by this fitting procedure not only the rate constant but also the coupling and the instrumental line width are determined. The resulting parameters of all the fittings are listed in *Tables 1* and *2*.

Table 1. *Rate Constants* k, *Coupling Constants* $J_{AX} = {}^1J(^{13}C,^6Li)$ *and Line-Width* $\Delta\nu$ *as Obtained from the Iterative Fit of the Spectra for* $^6Li^{13}CHBr_2$ (**1**) *Recorded at Various Temperatures.* $R = 100\,[\Sigma(y_i(\text{calc.}) - y_i(\text{exp.}))^2/\Sigma y_i^2(\text{exp.})]^{1/2}$.

T [°]	k[a]) [$l \cdot mol^{-1}s^{-1}$]	J_{AX} [Hz]	$\Delta\nu$ [Hz]	R factor
− 95.8	746.0	15.1	6.66	6.4
− 99.2	476.0	15.9	7.54	4.2
− 101.8	293.0	16.1	7.83	3.6
− 103.8	250.0	16.6	7.34	4.4
− 104.8	185.0	16.7	5.48	7.1
− 107.8	101.0	16.7	5.92	5.0
− 112.0	36.4	16.9	6.33	7.6
− 116.7	15.3	16.8	6.82	4.6

[a]) From the relation $1/\tau_{AX} = k[AX]$; [AX] = 0.15M, see *Appendix D*.

Table 2. *Optimized Rates* k, *Coupling Constants* $J_{AX} = {}^1J(^{13}C,^6Li)$ *and Line-Width* $\Delta\nu$ *for* $C_6H_5S^{13}CH_2^6Li$ (**2**) *at Various Temperatures. R* factor as defined in *Table 1*.

T [°]	k[a]) [$l \cdot mol^{-1}s^{-1}$]	J_{AX} [Hz]	$\Delta\nu$ [Hz]	R factor
− 100.0	1220	12.8	5.41	6.6
− 107.2	328	10.7	6.47	4.0
− 112.4	128	10.6	6.84	4.1
− 117.6	27.0	10.7	8.57	4.7
− 123.0	[−2.2]	10.6	10.8	3.1
− 127.4	[−1.1]	10.7	13.2	2.2
− 132.7	[12.6]	11.8	16.6	2.9

[a]) From the relation $1/\tau_{AX} = k[AX]$; [AX] = 0.15M.

Fig. 2 reproduces the *Eyring* plots constructed for compounds **1** (white circles) and **2** (black circles) using the rates reported above; the least-squares-optimized (using program NMRACP [8]) activation parameters are listed in *Table 3*.

The quadrupolar-relaxation model for spin 1 (^{6}Li has spin 1) as in [9] could also explain the temperature dependence of the spectra of **1** and **2**. In fact, very good fits between experimental and calculated spectra could be obtained by optimizing all parameters implied in this relaxation model. However, the quadrupolar relaxation can not account for the dependence of the line shape upon concentration as observed for **2**; furthermore, in the case of **1**, the fits of the line-shape at the highest temperatures lead to unrealistic values for the coupling constant $^1J(^{13}C,^6Li)$ (decreasing from 16.3 to 13.8 Hz). We have, therefore, abandoned the quadrupolar-relaxation model and given our preference to the spin-exchange mechanism.

Table 3. *Activation Parameters of* **1** *and* **2**[a]) (see *Scheme 1*)

	$LiCHBr_2$ (**1**)	$LiCH_2SC_6H_5$ (**2**)
E_a	10.6 ± 1.4 kcal/mol	11.4 ± 1.5 kcal/mol
$\log A$	16.0 ± 1.8	17.5 ± 2.0
$\Delta H^{\neq}$	10.2 ± 1.4 kcal/mol	11.1 ± 1.5 kcal/mol
$\Delta S^{\neq}$	13.7 ± 9.9 cal/mol·K	20.6 ± 9.5 cal/mol·K
$\Delta G^{\neq}$ (25°)	6.16 ± 0.2 kcal/mol	4.89 ± 0.2 kcal/mol

[a]) The temperature errors ($\Delta T_1 = \Delta T_2 = 1$ K) affecting the lowest and highest recording temperature as well as the deviations of the corresponding rates ($\Delta k_1/k_1 = \Delta k_2/k_2 = 0.3$) estimated from spectra fits are used to calculate the errors [8] given. These errors are more realistic than the statistical errors deduced solely from the least-squares regression.

The value of $\Delta S^{\neq}$ is worth to be discussed here. For bimolecular reactions in solutions a value of $\Delta S^{\neq}$ between 7 and 12 cal/mol·K is to be expected [10]. (Note that the very high value reported for $\Delta S^{\neq}$ in *Table 3* have in fact to be increased by $R \cdot \ln 2$ since the rate for reaching the transition state from any pairs of monomers is $k_1 = 2k$.) The high $\Delta S^{\neq}$ value must result from the fact that two THF molecules are released when two monomeric species react to form a dimer. In the transition state of such a process, either the two THF molecules are completely released and so $\Delta S^{\neq}$ must contain the corresponding translational and rotational contributions, or the THF molecules are much more weakly bonded then in the monomers and, therefore, very low frequency vibration could contribute to $\Delta S^{\neq}$. The $\Delta S^{\neq}$ must, therefore, be greater than the expected pure bimolecular values of 7 to 12 cal/mol·K.

3. Line-Shape Analysis of the Spectra of $^6Li^{13}CH_2C_3H_7$ (3). – At −30°, hexane-free solutions of ^{13}C-labelled (^6Li)butyllithium (**3**) in (D_8)THF show a broad, unresolved ^{13}C-NMR signal (10.8 ppm) [3a] [3e] which upon cooling down to −100° splits into two signals, a broad one flanked by a resolved quintuplet ($^1J(^{13}C,^6Li) = 7.8$ Hz). The quintuplet must arise from the dimeric species **3b**, and the unresolved signal has to be assigned to the tetramer **3a**. Integration of the two signals indicates that the dimer (12.4 ppm) to tetramer (10.4 ppm) ratio approaches 1:1 at low temperatures. As is evident from *Fig. 3*, the broad signal of the dimer measured at −88° becomes better resolved upon dilution of the solution (from 0.5 to 0.16M) and, as verified by integration, it also increases in intensity with respect to the signal of the tetramer. From integrations of the signals recorded at different temperatures and different global concentrations, the dimer/tetramer ratios and, therefore, the 'pseudo'-equilibrium constants and the thermodynamic parameters for the reaction formulated in *Scheme 2* could be obtained. They are reproduced in *Table 4*.

To analyse the dynamic behaviour of BuLi, we first assume that there is an intermolecular exchange between dimer **3b** and tetramer **3a** according to the most obvious model shown in *Scheme 3*. In view of the large number of wave functions necessary for treating the full spin system[1]) $B^1B^2B^3B^4Y^1Y^2Y^3Y^4$ (compare the $2^4 \cdot 3^4 = 1296$ wave functions with the $2^1 \cdot 3^1 = 6$ wave functions in the foregoing examples of **1** and **2**, *Scheme 1*), any analysis – without the help of a powerful algebraic formula manipulating program –

[1]) Since we have to use indices for every spin, we abandoned the usual notation B′B″B‴B⁗Y′Y″Y‴Y⁗ in favour of the one given here.

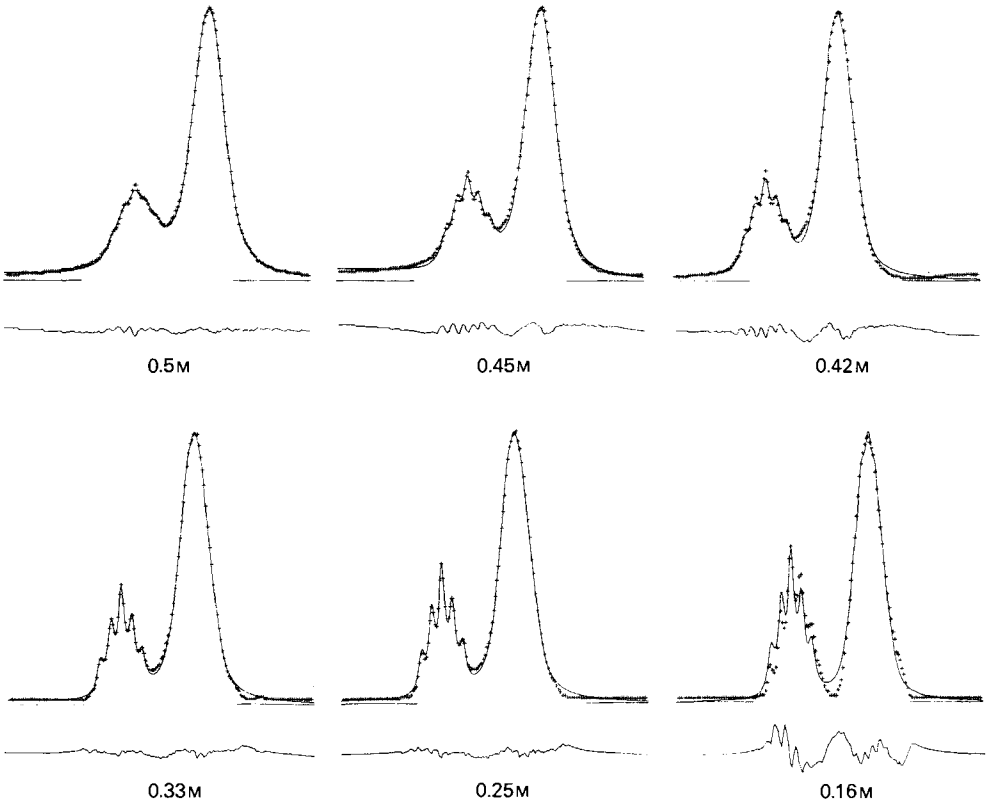

Fig. 3. *Comparison of the measured* [3e] *(+) and calculated line-shape of the* $^6Li^{13}CH_2C_3H_7$ *(3)* ^{13}*C-NMR signal at different concentrations at* $-88°$. The errors y_i(calc.) – y_i(exp.) are plotted in the same intensity scale below the spectra.

Scheme 2

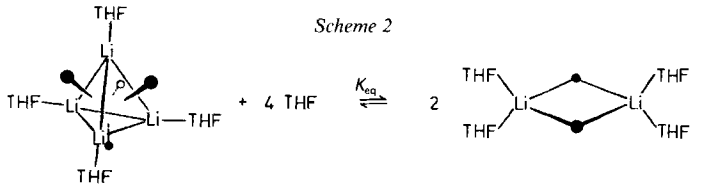

(2)

3a **3b**

● = $^{13}CH_2C_3H_7$; $K'_{eq} = [\mathbf{3b}]^2/[\mathbf{3a}] = K_{eq}\,[THF]^4$

is completely out of the question. Another acceptable model, shown in *Scheme 4*, according to which tetramers are formed and deaggregated (*via* a hexameric transition state) led to a simpler spin-exchange formalism; the corresponding density matrix deduced is outlined in *Appendix C*. Once again, the kinetic results have been obtained by fitting the digitalized spectra using the programs NMREX2 *(Table 5)* and NMRACP. Both, the concentration-dependent spectra and the temperature-dependent spectra of **3** [3a] could be nicely

Table 4. *Experimental Data, Equilibrium Constants and Thermodynamic Data of* **3** [3e]

[BuLi] [mol/l]	Normalized integrals D and T of the ^{13}C-NMR signals of **3b** and **3a**, resp., at three temperatures						$K'_{eq} \cdot 10^{2a}$) [mol/l]		
	−87.8°		−69.1°		−50.7°		−87.8°	−69.1°	−50.7°
	D	T	D	T	D	T			
0.50	0.255	0.745	0.204	0.796	0.106	0.894	4.36	2.61	0.630
0.45	0.243	0.757	0.200	0.800	0.103	0.897	3.51	2.25	0.530
0.42	0.247	0.753	0.216	0.784	0.129	0.871	3.40	2.50	0.800
0.33	0.275	0.725	0.174	0.826	0.117	0.883	3.44	1.21	0.510
0.25	0.298	0.702	0.202	0.798	0.148	0.852	3.16	1.28	0.640
0.16	0.352	0.648	0.246	0.754	0.178	0.822	3.06	1.28	0.620
0.10	0.410	0.590	0.308	0.692	0.240	0.760	2.85	1.37	0.760

[a]) Calculated by means of $K'_{eq} = [BuLi]\, D^2/T$. $\Delta H_R = -3.65 \pm 1.3$ kcal/mol, $\Delta S_R = -26.3 \pm 6.9$ cal/mol·K, and $\Delta G_R(-88°) = 1.21 \pm 0.84$ kcal/mol. The errors given for ΔH_R, ΔS_R, and ΔG_R are based on $\Delta K'_{eq}/K'_{eq} = 0.5$.

Scheme 3

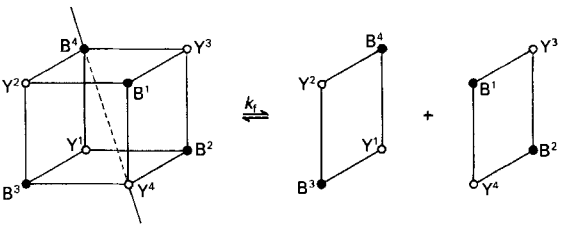

$B^1B^2B^3B^4Y^1Y^2Y^3Y^4 \rightleftharpoons B^3B^4Y^1Y^2 + B^1B^2Y^3Y^4$ (3a)

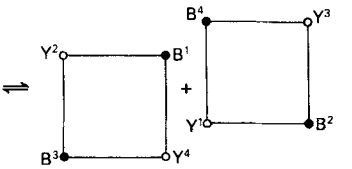

$\rightleftharpoons B^1B^3Y^2Y^4 + B^2B^4Y^1Y^3$ (3b)

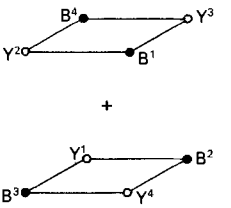

$\rightleftharpoons B^1B^4Y^2Y^3 + B^2B^3Y^1Y^4$ (3c)

Scheme 4

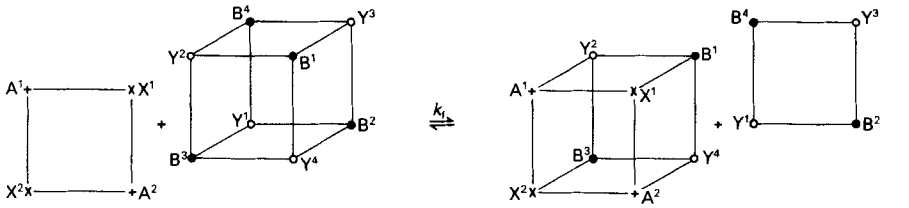

$A^1A^2X^1X^2 + B^1B^2B^3B^4Y^1Y^2Y^3Y^4 \rightleftharpoons A^1A^2B^1B^3X^1X^2Y^2Y^4 + B^2B^4Y^1Y^3$ (4a)

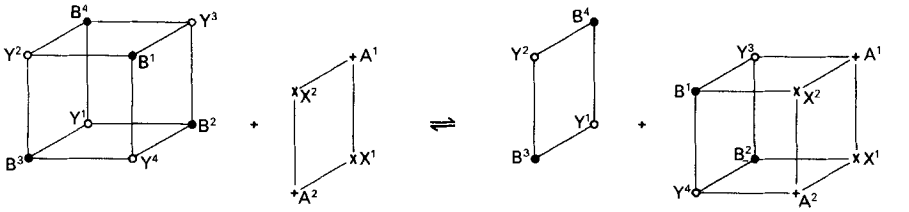

$B^1B^2B^3B^4Y^1Y^2Y^3Y^4 + A^1A^2X^1X^2 \rightleftharpoons B^3B^4Y^1Y^2 + A^1A^2B^1B^2X^1X^2Y^3Y^4$ (4b)

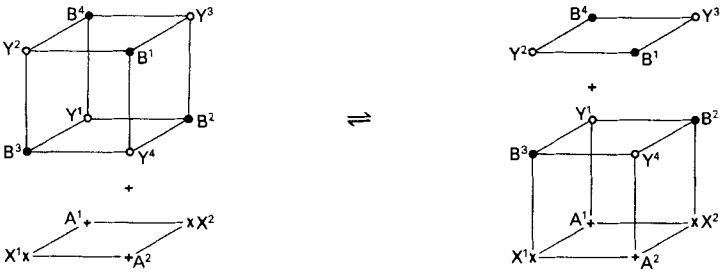

$A^1A^2X^1X^2 + B^1B^2B^3B^4Y^1Y^2Y^3Y^4 \rightleftharpoons B^1B^4Y^2Y^3 + A^1A^2B^2B^3X^1X^2Y^1Y^4$ (4c)

matched by calculation (*Fig. 3* shows spectra of **3** recorded at −88° at different concentrations). The fittings lead to the values of K_{eq}, ΔG_R, ΔH_R, and ΔS_R (*Table 6*, for details, see *Appendix E*) which are in good agreement with those obtained from simple integration (*Table 4*); the equilibrium constant calculated by extrapolation at −108° was further confirmed by cryoscopic determination of the degree of aggregation of BuLi in freezing THF [7]. The *Eyring* plot (*Fig. 4*) is constructed from the rates given in *Table 5*; the corresponding activation parameters are reported in *Table 6*.

Discussion of the Results Obtained for (^{6}Li)Butyllithium (**3**). The mathematical and computational efforts devoted to the analysis of the dynamic behaviour of **3** may look exaggerated. One has to point out here that half of the atoms considered in the exchange

Table 5. *Optimized Parameters of Intermolecular Exchange of Dimer* **3b** *and Tetramer* **3a**

[BuLi]	t	Dimer				Tetramer					Results				
		Ca[a])	ν_A[b])	J''	$\Delta\nu_A$[c])	CB[a])	ν_B[b])	J	J'[d])	$\Delta\nu_B$[c])	$1/\tau_A$	$1/\tau_B$	k_f[e])	R[f])	$K'_{eq}\cdot 10^2$[g])
[mol/l]	[°]		[Hz]	[Hz]	[Hz]		[Hz]	[Hz]	[Hz]	[Hz]	[s^{-1}]	[s^{-1}]	[l/mol·s]		[mol/l]
0.18[h])	−110	0.324	315.2	8.93	7.74	0.676	248.9	4.10	[0.2][i])	26.36	0.147	0.142	4.87	5.0	2.80
0.18[h])	−100	0.292	316.1	8.94	5.49	0.708	251.2	4.22	[0.2]	22.85	0.322	0.266	10.1	4.7	2.17
0.18[h])	−90	0.264	317.5	7.83	3.69	0.736	262.3	4.66	[0.2]	13.59	0.500	0.358	15.1	3.1	1.70
0.5	−87.8	0.230	317.3	8.89	[11.00]	0.770	261.0	5.45	[0.2]	15.45	1.71	1.03	17.8	2.0	3.44
0.45	−87.8	0.224	317.1	8.54	[6.00]	0.766	261.3	5.18	[0.2]	13.94	2.01	1.16	23.0	4.1	2.91
0.42	−87.8	0.251	318.7	8.42	7.52	0.749	262.7	5.70	[0.2]	10.43	1.52	1.01	19.3	4.9	3.53
0.33	−87.8	0.233	318.8	7.89	5.16	0.767	262.8	5.43	[0.2]	10.91	1.15	0.704	18.3	3.1	2.34
0.25	−87.8	0.261	319.3	7.85	5.08	0.739	262.9	5.41	[0.2]	10.75	0.844	0.596	18.3	3.5	2.31
0.16	−87.8	0.310	319.1	7.74	5.45	0.690	259.8	5.46	[0.2]	8.10	0.515	0.465	18.7	10.5	2.24
0.5	−69.1	0.144	315.9	7.61	[4.00]	0.856	260.7	5.11	[0.2]	13.78	4.84	1.62	45.2	2.1	1.20
0.45	−69.1	0.171	315.7	7.74	[4.00]	0.829	261.2	5.65	[0.2]	10.00	4.11	1.71	44.2	3.2	1.59
0.25	−69.1	0.190	315.2	6.36	[3.68]	0.810	261.0	5.69	[0.2]	7.61	2.25	1.06	44.5	4.3	1.11
0.5	−50.1	0.093	312.1	6.48	[4.00]	0.907	260.5	4.28	[0.2]	17.09	10.7	2.17	94.0	1.0	0.475
0.45	−50.1	0.112	311.8	2.82	[4.00]	0.888	260.0	4.82	[0.2]	13.36	9.13	2.31	91.4	2.1	0.631
0.25	−50.1	0.153	312.6	3.24	[4.00]	0.847	260.2	5.22	[0.2]	7.72	7.82	2.83	148	2.9	0.692
0.18[h])	−30	[0.180]	[316.1]	[7.20]	[4.00]	[0.820]	261.5	[5.20]	[0.2]	8.11	20.5	9.00	556	4.2	0.710

[a]) Normalized integrals CA and CB of the dimer and tetramer, respectively.
[b]) Resonance frequencies as used in the computations.
[c]) Instrumental line-widths adjusted by least-squares.
[d]) Guessed long-range coupling constant.
[e]) $k_f = 4(1/\tau_A)/(CB\cdot[BuLi]) = 2(1/\tau_B)/(CA\cdot[BuLi])$.
[f]) R factor (see *Table 1*).
[g]) $K'_{eq} = [BuLi]\,(CA)^2/CB$.
[h]) From [3a].
[i]) Parameters in square brackets had been kept constant during the iterations.

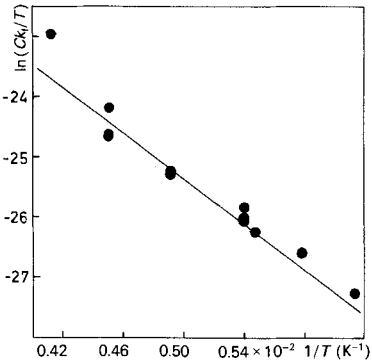

Fig. 4. Eyring *plot of the rates* k_f *of the intermolecular exchange of dimer* **3b** *and tetramer* **3a**. $C = h/k_b$ (as in *Fig. 2*).

Table 6. *Thermodynamic Data and Activation Parameters for the Reaction* **3a**→2 **3b**[a])

		E_a	= 4.18 ± 0.65 kcal/mol
		$\log A$	= 6.21 ± 0.73
ΔH_R	= −2.06 ± 1.1 kcal/mol	$\Delta H^{\neq}$	= 3.78 ± 0.64 kcal/mol
ΔS_R	= −18.8 ± 4.4 cal/mol·K	$\Delta S^{\neq}$	= −31.3 ± 4.2 cal/mol·K
ΔG_R (−88°)	= 1.42 ± 0.90 kcal/mol	$\Delta G^{\neq}$ (25°)	= 13.11 ± 0.33 kcal/mol

[a]) The errors of ΔH_R, ΔS_R, and ΔG_R are based on $\Delta T_1 = \Delta T_2 = 2$ K and $\Delta K'_{eq}/K'_{eq} = 0.5$. Those of the activation parameters result from $\Delta T_1 = \Delta T_2 = 2$ K and $\Delta k_f/k_f = 0.5$ (compare remarks in *Table 3*).

processes have spin 1 and that there is no simple way to analyse in detail the ^{13}C-NMR spectra other than the one used here. Note that some simplifications were introduced; for instance, we did not take into account quadrupolar relaxation effects due to ^{6}Li (see *Appendix A*).

In the absence of any exchange, the tetramer **3a** is expected to give seven lines (neglecting the long-range coupling); the fact that the tetramer signal exhibits no fine structure neither upon dilution nor by temperature decrease is not explained in our analysis; we have simulated this fact using a larger line-width value. A dynamic process must, however, be responsible for the line-shape of the tetramer signal at very low temperature; for instance, a rotation of a 'dimer face' with respect to the other face [4a] [4b] *(Scheme 5)* in the tetramer itself could explain the extra broadening of the tetramer peak observed at low temperatures. As indicated by the data in *Table 5*, it seems that a coupling averaging process also takes place in the dimer at temperatures higher than −70°

Scheme 5

$B^1B^2B^3B^4Y^1Y^2Y^3Y^4 \rightleftharpoons B^1B^2B^3B^4Y^1Y^4Y^3Y^2$

(in our computations both line-width and J'' are self-adjusting parameters). In view of the relatively low spectral information contained in the high-temperature spectra, a more elaborate exchange mechanism would not be worthwhile to be developed. Even with the exchange matrix given in *Appendix C* (see *Fig. 6*) there are enough adjustable parameters to render the determination of the rate constant rather cumbersome.

Comment on the Thermodynamic Parameters for the Reaction (BuLi)$_4$·4 THF + 4 THF → 2 (BuLi)$_2$·4 THF. Our ΔH_R values reported in *Tables 4* and *6* refer to the equation above and are in good agreement with the thermodynamic titration value which we have estimated from the diagram shown in [2a] to be −3.6 kcal/mol. The strongly negative ΔS_R value is in agreement with the proposed stoichiometry of the reaction. The value reflects the loss of translational and rotational degrees of freedom of four molecules of THF. This should amount to about -10 R = -20 cal/mol·K. The characteristics of the dynamic equilibrium between the dimer and the tetamer lies in the fact that both ΔS_R and $\Delta S^{\neq}$ are strongly negative while ΔH_R and $\Delta H^{\neq}$ are small. *Fraenkel et al.* [2b] have obtained very similar values for $\Delta H^{\neq}$ and $\Delta S^{\neq}$ ($\Delta H^{\neq}$ = 4.3 kcal/mol and $\Delta S^{\neq} = -36$ cal/mol·K) in the case of exchange of alkyl groups and Li-atoms among aggregates of propyllithium in cyclopentane.

In the meantime, *McGarrity et al.* [12] have reported thermodynamic parameters ($\Delta H_R = -1.5$ kcal/mol and $\Delta S_R = -13.8$ cal/mol·K) derived from ^{7}Li-NMR spectra for the equilibrium dimer/tetramer of **3** in THF; their results are in agreement with ours; however, their activation parameters ($\Delta G^{\neq}$ (25°) = 11.95 kcal/mol, $\Delta H^{\neq}$ = 9.80 kcal/mol, and $\Delta S^{\neq} = -7.2$ cal/mol·K) differ appreciably from ours.

4. Conclusion. – The line-shape analysis of temperature- and concentration-dependent ^{13}C-NMR signals of compounds **1**–**3** containing ^{6}Li-metalled C-atoms has provided activation parameters and – in part – equilibrium parameters for reactions occurring between monomers, dimers, and/or different aggregates. It turns out that the dynamic processes under discussion are fast even at the lowest temperatures (−75 to −120°) at which the investigated reagents dibromomethyllithium, phenylthiomethyllithium, and butyllithium are usually employed in synthetic applications. In view of the results described here, it is not surprising that open-chain Li-compounds metallated at a center of chirality do not exhibit configurational stability (exceptions are cyclic and α-RO-substituted open-chain derivatives) [11]. The results obtained also suggest that special techniques are required if one wishes to find out which of the species present in equilibrium is really involved in the product-forming reaction step when an electrophile is added to the Li-compound. Rapid reagent mixing techniques assisted with fast NMR-spectroscopic analysis as developed by *McGarrity et al.* [12] seems to be a promising experimental approach to obtain informations about the mechanisms of such reactions.

We thank Dr. *R. Hässig* for carrying out the so far unpublished [3e] concentration-dependent measurements of labelled butyllithium which were used for the present line-shape analysis.

Appendix A. – *Derivation of the Density-Matrix Equations (Case of* **1** *and* **2**). The density-matrix equations (in the product representation) were derived using the permutation of indices (PI) method described by *Kaplan* and *Fraenkel* [5]. The product functions for a spin system AX (spin of A = 1/2, spin of X = 1) are:

	a	x	$a + x$
1	1/2	1	3/2
2	1/2	0	1/2
3	− 1/2	1	
4	1/2	− 1	− 1/2
5	− 1/2	0	
6	− 1/2	− 1	− 3/2

In the ^{13}C-NMR spectra (^{13}C = A), the three transitions 1–3, 2–5, 4–6 for which the spin states of X do not change (first-order weak-coupling condition) are observed. According to [5], the exchange operator for the dynamic process corresponding to *Eqn. 1* can be written as

$$\tilde{\rho}^{AX}_{ax,a'x}(\text{after}) = \sum_{by} \tilde{\rho}^{AY}_{ay,a'y}\,\tilde{\rho}^{BX}_{bx,bx} = \sum_{b} \tilde{\rho}^{BX}_{bx,bx} \sum_{y} \tilde{\rho}^{AY}_{ay,a'y}, \tag{5}$$

$$\tilde{\rho}^{AY}_{ay,a'y}(\text{after}) = \sum_{bx} \tilde{\rho}^{AX}_{ax,a'x}\,\tilde{\rho}^{BY}_{by,by} = \sum_{b} \tilde{\rho}^{BY}_{by,by} \sum_{x} \tilde{\rho}^{AX}_{ax,a'x}. \tag{6}$$

For condition of low rf power, the diagonal density matrix elements can be approximated by $\tilde{\rho}^{AX}_{ax,ax} = 1/n_{AX}$ where n_{AX} is the dimension of the spin space ($n_{AX} = 6$); accordingly $\sum_{b} \tilde{\rho}^{BX}_{bx,bx} = \tilde{\rho}^{BX}_{\alpha x,\alpha x} + \tilde{\rho}^{BX}_{\beta x,\beta x} = 1/3$ noting that BX and AX are both monomers. The density-matrix elements corresponding to BY and BX are not needed since they would be identical to those of AX and AY.

To avoid unnecessary complications, we shall neglect quadrupolar relaxation due to spin 1 of ^{6}Li and use only the first-order *Hamiltonian*

$$\tilde{\mathscr{H}}^{AX}_{o} = (\omega^{AX}_{oA} - \omega)\,I_{1z} + (\omega^{AX}_{oX} - \omega)\,I_{2z} + J\,I_{1z}I_{2z}. \tag{7}$$

$-i(A+J)$ $-\frac{1}{T}-\frac{1}{\tau}$			$\frac{1}{3\tau}$	$\frac{1}{3\tau}$	$\frac{1}{3\tau}$	$\tilde{\rho}_{1,3}$	$\frac{1}{3}$
	$-i(A)$ $-\frac{1}{T}-\frac{1}{\tau}$		$\frac{1}{3\tau}$	$\frac{1}{3\tau}$	$\frac{1}{3\tau}$	$\tilde{\rho}_{2,5}$	$\frac{1}{3}$
		$-i(A-J)$ $-\frac{1}{T}-\frac{1}{\tau}$	$\frac{1}{3\tau}$	$\frac{1}{3\tau}$	$\frac{1}{3\tau}$	$\tilde{\rho}_{4,6}$	$\frac{1}{3}$
$\frac{1}{3\tau'}$	$\frac{1}{3\tau'}$	$\frac{1}{3\tau'}$	$-i(A'+J')$ $-\frac{1}{T'}-\frac{1}{\tau'}$			$\tilde{\rho}'_{1,3}$	$\frac{1}{3}$
$\frac{1}{3\tau'}$	$\frac{1}{3\tau'}$	$\frac{1}{3\tau'}$		$-i(A')$ $-\frac{1}{T'}-\frac{1}{\tau'}$		$\tilde{\rho}'_{2,5}$	$\frac{1}{3}$
$\frac{1}{3\tau'}$	$\frac{1}{3\tau'}$	$\frac{1}{3\tau'}$			$-i(A'-J')$ $-\frac{1}{T'}-\frac{1}{\tau'}$	$\tilde{\rho}'_{4,6}$	$\frac{1}{3}$

$= \beta' \frac{i}{2}$

Fig. 5. *System of linear equations determining the density-matrix elements* $\tilde{\rho}_{k,l}$ *for the intermolecular exchange corresponding to* Eqn. 1. $A = \omega^{AX}_{A}$, $A' = \omega^{AY}_{A}$; $1/T = 1/T_{AX}$, $1/T' = 1/T_{AY}$; $1/\tau = 1/\tau_{AX}$, $1/\tau' = 1/\tau_{AY}$. The transition probabilities are proportional to 1/3. $\beta' = (1/2)h\omega_1\omega_o/kT$; $\omega_o = \gamma H_o$, $\omega_1 = \gamma H_1$.

We are now able to construct the system of six linear equations which determine the density-matrix elements $\tilde{\rho}^{AX}_{ax,a'x}$ (and $\tilde{\rho}^{AY}_{ay,a'y}$) by applying the master equation as explained in [5]:

$$i\left[\sum_{kl}\tilde{\rho}^{AX}_{ax,kl}\langle kl|\tilde{\mathscr{H}}^{AX}_{o}|a'x\rangle - \sum_{mn}\langle ax|\tilde{\mathscr{H}}^{AX}_{o}|mn\rangle\tilde{\rho}^{AX}_{mn,a'x}\right] + \frac{1}{\tau_{AX}}\left[\tilde{\rho}^{AX}_{ax,a'x}(after) - \tilde{\rho}^{AX}_{ax,a'x}\right] - \frac{\tilde{\rho}^{AX}_{ax,a'x}}{T_{AX}} = \beta'\frac{i}{n_{AX}}\langle ax|\sum_{i}(I_i^+ - I_i^-)|a'x\rangle \tag{8}$$

(for $\tilde{\rho}^{AY}_{ay,a'y}$ substitute the indices X by Y and x by y).

If we have, for instance, $ax = \frac{1}{2}\ 1$ and $a'x = -\frac{1}{2}\ 1$ we get for the first linear equation

$$\left\{i\left[-(\omega^{AX}_{oA} - \omega) - J\right] - 1/\tau_{AX} - 1/T_{AX}\right\}\tilde{\rho}^{AX}_{1,3} + (1/\tau_{AX})(1/3)\left[\tilde{\rho}^{AY}_{1,3} + \tilde{\rho}^{AY}_{2,5} + \tilde{\rho}^{AY}_{4,6}\right] = \beta'\frac{i}{6}$$

The other five linear equations are obtained in the same way. This system of linear equations is reported in matrix form in *Fig. 5*.

Appendix B. – *Brief Description of Program NMREX2.* The program NMREX2 accepts matrices and vectors (in algebraical form) as, for instance, given in *Fig. 5*. The input consists of a block of constants and options in arbitrary sequence labelled by three characters, a title card, parameters labelled by two characters, the matrix in algebraical form, base-line shift, base-line tilt, least-squares monitoring parameters, a vector indicating which of the parameters should be varied, and the y_i values of the equally spaced digitalized data points. The program then proceeds (in a similar way as the program CNMREX which has been described earlier [8]) by diagonalizing the non-hermitian matrix **A** (for instance that given in *Fig. 5*) and computing the line shape:

$$y(\omega) = -S\,Re[\mathbf{C}^T\mathbf{U}(\boldsymbol{\Lambda} - i\omega\mathbf{E})^{-1}\mathbf{U}^{-1}\mathbf{B}] \tag{9}$$

where S = scaling factor, **C** = (concentration of species 1, concentration of species 2, ...), $\boldsymbol{\Lambda} = \mathbf{U}\mathbf{A}\mathbf{U}^{-1}$, and **B** = relative intensities of the transitions. The program then fits iteratively the experimental data, making use of the SPIRAL algorithm [8] [14]. Although not yet required (and not yet retested), the program contains data-correlation possibilities similar to that introduced by *Binsch* and *Stephenson* for static NMR analysis [15].

Appendix C. – *Derivation of the Density-Matrix Equations (case of* **3***).* Since we observe the ^{6}Li-splittings at site A(B), the first-order *Hamiltonian* for spin systems $A^1A^2X^1X^2$ and $B^1B^2B^3B^4Y^1Y^2Y^3Y^4$ can be written without loss of generality as follows (noting that $B^1 = B^2 = B^3 = 0$, $A^2 = 0$; the numbering being as given in *Scheme 4*):

$$\tilde{\mathscr{H}}^{AX_2}_{o} = (\omega_{oA} - \omega)I^z_A + (\omega_{oX} - \omega)I^z_X + J''I^z_AI^z_X \tag{10}$$

$$\tilde{\mathscr{H}}^{BY_4}_{o} = (\omega_{oB} - \omega)I^z_{b_4} + (\omega_{oY} - \omega)I^z_Y + JI^z_{b_4}(I^z_{y_1} + I^z_{y_2} + I^z_{y_3}) + J'I^z_{b_4}I^z_{y_4} \tag{11}$$

where $I^z_X = I^z_{x_1} + I^z_{x_2}$, $I^z_Y = I^z_{y_1} + I^z_{y_2} + I^z_{y_3} + I^z_{y_4}$.

Similarly to *Appendix A*, the exchange operators corresponding to *Eqn. 4a (Scheme 4)* are:

$$\tilde{\rho}^{B^4Y^1Y^2Y^3Y^4}_{b_4y_1y_2y_3y_4,b_4y_1y_2y_3y_4}(after) = \sum_{a_1x_1x_2}\tilde{\rho}^{A^1X^1X^2Y^2Y^4}_{a_1x_1x_2y_2y_4,a_1x_1x_2y_2y_4}\tilde{\rho}^{B^4Y^1Y^3}_{b_4y_1y_3,b_4y_1y_3} \tag{12}$$

$$\tilde{\rho}^{A^1X^1X^2}_{a_1x_1x_2,a_1x_1x_2}(after) = \sum_{b_4y_1y_2y_3y_4}\tilde{\rho}^{A^1X^1X^2Y^2Y^4}_{a_1x_1x_2y_2y_4,a_1x_1x_2y_2y_4}\tilde{\rho}^{B^4Y^1Y^3}_{b_4y_1y_3,b_4y_1y_3}. \tag{13}$$

Using the *s*elective *n*eglect *o*f *b*ilinear terms (SNOB) approximation [5], we obtain

$$\tilde{\rho}^{B^4Y^1Y^2Y^3Y^4}_{b_4y_1y_2y_3y_4,b_4y_1y_2y_3y_4}(after) = \frac{2\cdot 3\cdot 3}{162}\tilde{\rho}^{B^4Y^1Y^3}_{b_4y_1y_3,b_4y_1y_3}. \tag{14}$$

$$\tilde{\rho}^{A^1X^1X^2}_{a_1x_1x_2,a_1x_1x_2}(after) = \frac{2\cdot 3\cdot 3}{18}\sum_{y_2y_4}\tilde{\rho}^{A^1X^1X^2Y^2Y^4}_{a_1x_1x_2y_2y_4,a_1x_1x_2y_2y_4}. \tag{15}$$

Similar exchange operators can be written for the exchanges implied by *Eqns. 4b* and *4c*. The master equation has been constructed as in *Appendix A* except that three equally probable exchanges have to be considered here. The dimension of the problem is in principle equal to the number of transitions: 81 transitions for the tetramer and 9 transitions for the dimer. However, the number of lines expected to be observed is 7 and 5, respectively. We have

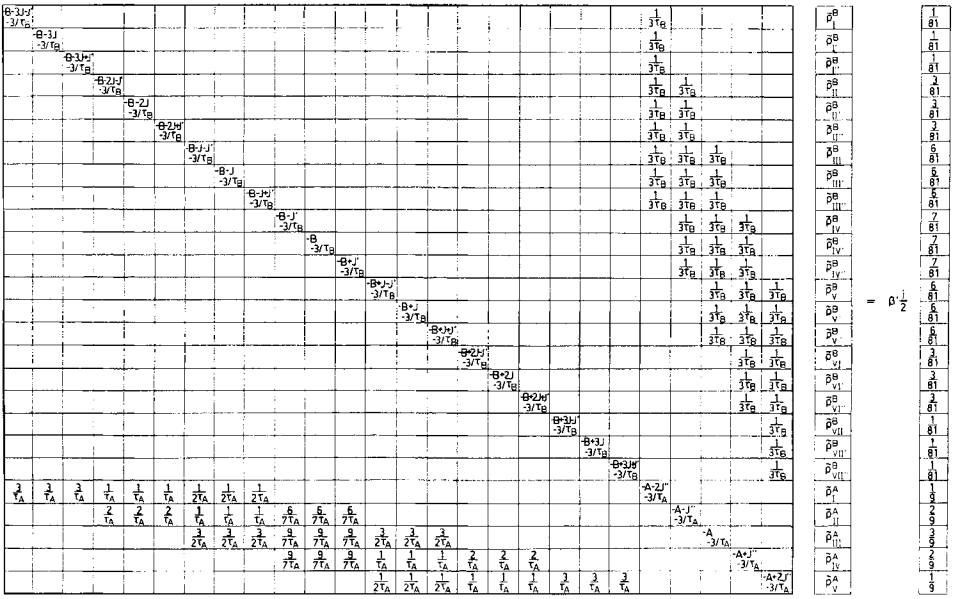

Fig. 6. *The exchange matrix* **A′** *describing the intermolecular exchange between dimers and tetramers of* **3** *corresponding to* Scheme 4. $A = \omega_{oA}$, $B = \omega_{oB}$; the terms containing the frequencies and couplings should be multiplied by $i = \sqrt{-1}$. τ_A = lifetime of dimer, τ_B = lifetime of tetramer. $1/T_A$ and $1/T_B$ had to be left out. β' is equal to that given in *Fig. 5*.

reduced the problem accordingly but we did not leave out the small coupling (J', over three bonds) expected to be present in the tetramer; the dimension was therefore reduced to 3 × 7 and 5; the final exchange matrix **A′** (see *Fig. 6*) could be written.

Appendix D. – *Kinetics of $LiCHBr_2$ and $LiCH_2SC_6H_5$.* In the steady-state approximation in which we consider the concentration of the intermediate [AXBY] as constant $d[AXBY]/dt = 0$, we have for the overall rate [10] as deduced from *Scheme 1*:

$$r = -d[AX]/dt = (k_1/2)[AX][BY] - (k_1/2)[AY][BX] = 0, \tag{16}$$

where k_1 is the rate constant for the reaction

$$2 \text{ monomers} \underset{k_1}{\overset{k_1}{\rightleftharpoons}} \text{dimeric intermediate} \rightleftharpoons 2 \text{ monomers}.$$

The mean preexchange lifetime τ_{AX} of one monomeric species in *Eqn. 1* is given by the relation [13]:

$$1/\tau_{AX} = (k_1/2)[AX][BY]/[AX] = (k_1/2)[BY]. \tag{17}$$

The factor 1/2 takes into account the fact that the dimeric intermediate can decompose in two ways.

Appendix E. – *Equilibrium Constant K_{eq} of the Reaction* **3a** ⇌ 2 **3b**. Since the concentration of THF implied in the reaction outlined in *Scheme 2* varies only very slightly (*Hässig* gives for [THF] a value of 13.57 mol/l [3e]), it seems best to use the 'pseudo'-equilibrium constant

$$K'_{eq} = [\mathbf{3b}]^2/[\mathbf{3a}] = K_{eq}\,[THF]^4$$

instead of K_{eq} for the evaluation of the thermodynamic data.

REFERENCES

[1] a) D.E. Appelquist, D.F. O'Brien, *J. Am. Chem. Soc.* **1963,** *85,* 743; b) A.W. Langer, *Trans. N. Y. Acad. Sci.* **1965,** *27,* 741; c) M. Szwarc, 'Carbanions, Living Polymers, and Electron Transfer Processes', Interscience, New York, 1968; d) E.A. Kovrizhnykh, A.I. Shatenshtein, *Russ. Chem. Rev.* **1969,** *38,* 840; e) J.M. Mallan, R.L. Bebb, *Chem. Rev.* **1969,** *69,* 693; f) P.D. Bartlett, C.V. Goebel, W.P. Weber, *J. Am. Chem. Soc.* **1969,** *91,* 7425; g) J.G. Carpenter, A.G. Evans, C.R. Gore, N.H. Rees, *J. Chem. Soc. B* **1969,** 908; h) C. Agami, *Bull. Soc. Chim. Fr.* **1970,** 1619; k) J.M. Brown, *Chem. Ind. (London)* **1972,** 454.

[2] a) R.P. Quirk, D.E. Kester, R.D. Delaney, *J. Organomet. Chem.* **1973,** *59,* 45; b) R.P. Quirk, D.E. Kester, *J. Organomet. Chem.* **1974,** *72,* C23.

[3] a) D. Seebach, R. Hässig, J. Gabriel, *Helv. Chim. Acta* **1983,** *66,* 308; b) R. Hässig, D. Seebach, *ibid.* **1983,** *66,* 2269; c) D. Seebach, J. Gabriel, R. Hässig, *ibid.* **1984,** *67,* 1083; d) J. Gabriel, Dissertation No. 7252, ETH Zürich, 1983; e) R. Hässig, Dissertation No. 7348, ETH Zürich, 1983.

[4] a) G. Fraenkel, A.M. Fraenkel, M.J. Geckle, F. Schloss, *J. Am. Chem. Soc.* **1979,** *101,* 4745; b) G. Fraenkel, M. Henrichs, J.M. Hewitt, B.M. Su, M.J. Geckle, *ibid.* **1980,** *102,* 3345; c) G. Fraenkel, P. Pramanik, *J. Chem. Soc., Chem. Commun.* **1983,** 1527.

[5] a) J.I. Kaplan, G. Fraenkel, *J. Am. Chem. Soc.* **1972,** *94,* 2907; b) J.I. Kaplan, G. Fraenkel, in 'NMR of Chemically Exchanging Systems', Academic Press, New York, 1980.

[6] a) R. Amstutz, Th. Laube, W.B. Schweizer, D. Seebach, J.D. Dunitz, *Helv. Chim. Acta* **1984,** *67,* 224; b) R. Amstutz, Dissertation No. 7210, ETH Zürich, 1983.

[7] W. Bauer, D. Seebach, *Helv. Chim. Acta* **1984,** *67,* 1972.

[8] J. Heinzer, J.F.M. Oth, *Helv. Chim. Acta* **1981,** *64,* 258, and lit. cited therein.

[9] J. Bacon, R.J. Gillespie, J.S. Hartman, U.R.K. Rao, *Mol. Phys.* **1970,** *18,* 561.

[10] F. Wilkinson, in 'Chemical Kinetics and Reaction Mechanisms', Van Nostrand Reinhold Company, New York, 1980.

[11] a) W.C. Still, *J. Am. Chem. Soc.* **1978,** *100,* 1481; W.C. Still, C. Sreekumar, *ibid.* **1980,** *102,* 1201; b) E.J. Corey, Th.M. Eckrich, *Tetrahedron Lett.* **1983,** *24,* 3163; c) E.J. Corey, G. Schmidt, K. Shimoji, *ibid.* **1983,** *24,* 3169.

[12] a) J.F. McGarrity, J. Prodolliet, T. Smith, *Org. Magn. Reson.* **1981,** *17,* 59; b) J.F. McGarrity, C.A. Ogle, *J. Am. Chem. Soc.* **1985,** *107,* 1805; c) J.F. McGarrity, C.A. Ogle, Z. Brich, H.-R. Loosli, *ibid.* **1985,** *107,* 1810.

[13] E. Grunwald, A. Loewenstein, S. Meiboom, *J. Chem. Phys.* **1957,** *27,* 630.

[14] a) A. Jones, *Comput. J.* **1970,** *13,* 301; b) D.S. Stephenson, G. Binsch, *J. Magn. Reson.* **1978,** *32,* 145; *ibid.* **1980,** *37,* 395 and 409.

[15] D.S. Stephenson, G. Binsch, *J. Magn. Reson.* **1980,** *37,* 395.